

論文 / 著書情報
Article / Book Information

論題(和文)	風荷重による振動を受ける複層粘弾性ダンパーの簡易モデル化手法
Title(English)	SIMPLIFIED MODELING APPROACH FOR MULTI-LAYERED VISCOELASTIC DAMPERS UNDER WIND-INDUCED VIBRATION
著者(和文)	梁其峻, 佐藤大樹, OSABEL Dave M.
Authors(English)	LIANG Qijun, SATO Daiki, OSABEL Dave Montellano
出典 / Citation	日本建築学会関東支部研究報告集, , , pp. 441-444
Citation(English)	, , , pp. 441-444
発行日 / Pub. date	2025, 3
権利情報	一般社団法人 日本建築学会

SIMPLIFIED MODELING APPROACH FOR MULTI-LAYERED VISCOELASTIC DAMPERS UNDER WIND-INDUCED VIBRATION

構造—振動

正会員 ○ 梁 其峻^{*1} 同 佐藤 大樹^{*2}
同 Osabel Dave M.^{*3}

Multi-layered viscoelastic (VE) damper, Wind-induced vibration, random wave

One-dimensional time-history analysis, Heat generation, Heat transfer analysis

1. INTRODUCTION

1.1. Viscoelastic damper

Viscoelastic (VE) damper is one of the effective damping components for high-rise buildings, as it can absorb vibration energy effectively not only from seismic-induced but also from wind-induced structural vibrations. It dissipates structural vibration through shear deformation of the VE material, then converts the absorbed energy into heat. Hence, its temperature can significantly increase.

Shown in Figs. 1a and 1b are the force-deformation ($F_d - u_d$) and the force-velocity ($F_d - \dot{u}_d$) hysteresis curves, respectively, of a VE damper subjected to harmonic loading. Their slopes are the storage stiffness K'_d and damping coefficient C_d , respectively. VE dampers exhibit complex property-change during vibrations due to their sensitivities to frequency, temperature, and strain level. As temperature increases or strain level becomes high during vibration, both storage stiffness K'_d and damping coefficient C_d decrease.

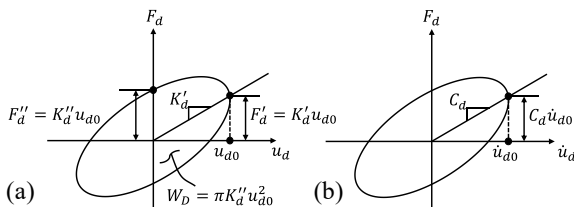


Figure 1. (a) $F_d - u_d$ and (b) $F_d - \dot{u}_d$ hysteresis curves.

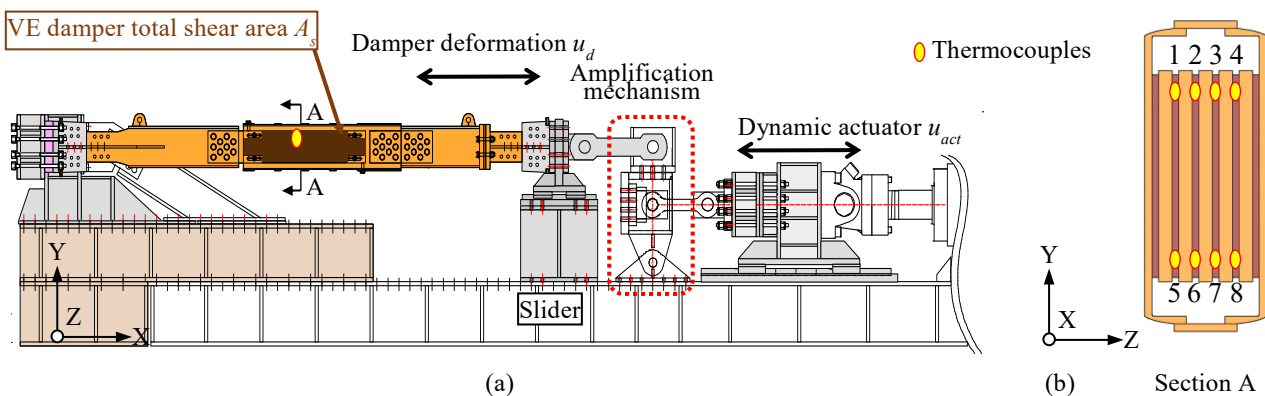


Figure 2. (a) Test setup of the six-layered VE damper and (b) locations of thermocouples.

These changes in K'_d and C_d become more complex under random loads such as wind loads, long-duration loading, and in multi-layered damper configurations.

1.2. Objective

The property changes of VE dampers have been extensively studied through various one-dimensional (1D) time-history methods [1-4]. However, these methods involve detailed element divisions and complex calculations, leading to significant computational loads in practical structural analyses.

Pursuant to these, this study aims to propose a simplified 1D modeling approach with high computational efficiency for analyzing multi-layered VE dampers. This modeling approach represents multiple VE layers with a simplified 1D model while maintaining accuracy. The proposed modeling approach is incorporated into the 1D time-history method that considers the temperature-, frequency-, and strain-level sensitivities of VE damper behavior. Based on the proposed modeling approach, this study carries out the 1D time-history method to simulate a wind-induced vibration test on a six-layered VE damper, aiming to validate the modeling approach's accuracy and effectiveness.

2. VE DAMPER TEST

This chapter presents the deformation-controlled loading test on VE damper from the Sato et al. study [5].

2.1. Test specimen and setup

Figs. 2a and 2b show the six-layered VE damper used in the test [5]. The damper is symmetrical in the XY - and XZ - planes. The dimensions of VE damper test specimen are length $l = 4024.5$ mm, thickness of one VE slab $d_v = 8$ mm, total shear area $A_s = 9120$ cm². The 3M-ISD111 type VE material used in this damper has the following properties: static shear modulus $G = 3.92$ N/cm², fractional derivative order $\alpha = 0.558$, temperature sensitive constants $a_{ref} = 0.000056$ and $b_{ref} = 2.10$ at reference temperature $\theta_{ref} = 20^\circ\text{C}$, $p_1 = 14.06$ and $p_2 = 97.32$.

Temperatures inside the damper at Section A (Fig. 2c) were measured during loading with 0.01 seconds intervals. The average values of eight thermocouple measurements will be presented and used as reference to evaluate analysis accuracy.

Figs. 3b and 3c show the wind-induced deformation time-histories used to apply to the VE damper in the test [5] and the following analysis in this study. The power spectral density (PSD) plots of these deformations (Fig. 3d) have peaks at natural frequency $f_0 = 0.333$ Hz, with along-wind direction containing more low frequency components. These were obtained from time-history analysis of a 200 m high building [5] with natural period = 3 seconds and damping ratio = 2%, subjected to wind loads with 500 years return period and roughness category III [6] (the mean component is set to zero to eliminate its unclear impact on VE damper properties and temperature rise). The obtained deformation time histories were normalized using a reference standard deviation of $\sigma_u = 4.0$ mm to achieve peak maximum deformation of about 16 mm (strain level = 200%).

3. VE DAMPER MODELING APPROACH

This chapter proposes a simplified modeling approach for multi-layered VE dampers by examining the temperature

distributions within VE slabs obtained from the 1D time-history analysis based on original detailed modeling approach.

3.1. Analysis of temperature distribution [4]

The temperature distributions within multi-layered VE dampers were first investigated using the detailed modeling approach [4], here refer as the original model. In the original model, each VE slab was divided into 12 elements to accurately capture the varying temperature distributions in thickness direction (Fig. 4a). For the details of the 1D time-history analysis method using the original model, please refer to Reference [4]. As shown in Fig. 5, the nodal temperatures distributed similarly in all three VE slabs during the loading period. This observation suggests that representing multiple VE slabs with a single VE slab could be a viable simplification approach.

3.2. Simplified modeling approach and analysis scheme

As shown in Fig. 4b, in the simplified modeling approach (referred to as the proposed model hereafter), the damper is represented by a single VE slab with one VE element, while maintaining the total shear area of 9120 cm² to ensure equivalent damping capacity compare with damper test specimen and the original model. This significant reduction in the number of elements and VE layers leads to great computational savings.

Considering the proposed model in Fig. 4b, the two VE nodes at the VE-to-steel interfaces are numbered as j_a and j_b . The 1D time-history analysis [4] can be carried out using the proposed model, implementing the VE constitutive rules [7, 8] to considers the temperature-, frequency-, and strain-level sensitivities of VE damper behavior. The flowchart for the proposed method is shown in Fig. 6. In the Material property calculation, the fractional derivative equation of order α can be written as

$$\tau_v^{(n)} + a_v^{(n)} D^\alpha \tau_v^{(n)} = G^{(n)} [\gamma_d^{(n)} + b_v^{(n)} D^\alpha \gamma_d^{(n)}]. \quad (1)$$

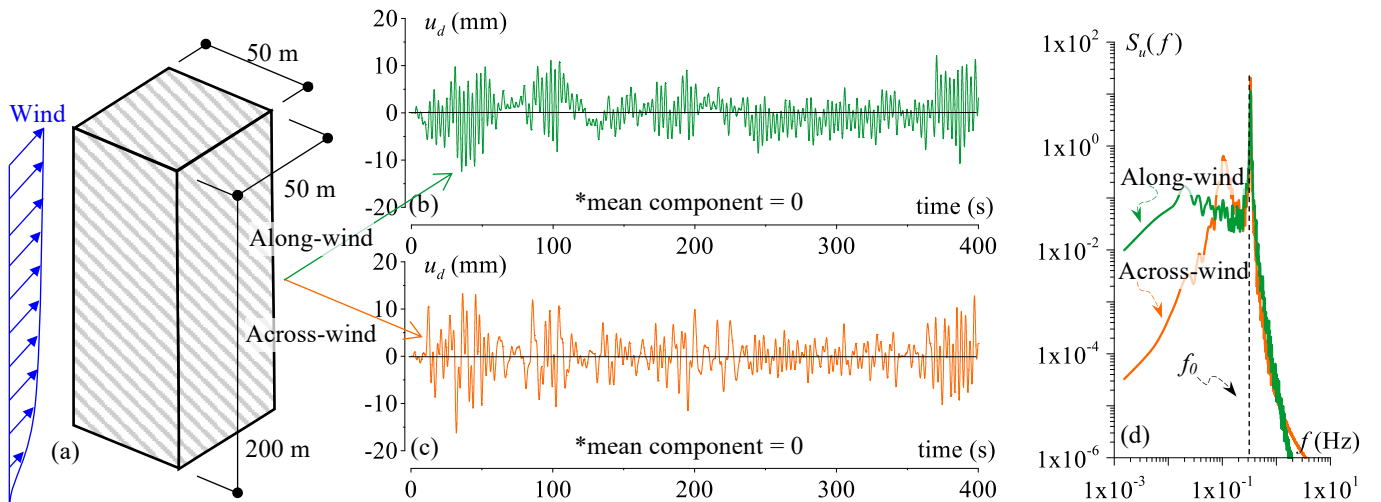


Figure 3. (a) Assumed building, (b and c) time-histories and (d) power spectral density of damper deformation in Along-wind direction and Across-wind direction.

The step-by-step integration of Eq. 1 results in:

$$\tau_v^{(n)} + a_v^{(n)} \sum_{i=0}^N w^{(n)} \tau_v^{(i)} = G^{(n)} [\gamma_d^{(n)} + b_v^{(n)} \sum_{i=0}^N w^{(n)} \gamma_d^{(i)}]. \quad (2)$$

Here, n = time step, $\tau_v^{(n)}$ = shear stress, w = weight factors and N = number of “window steps” for integration. The parameters of the fractional derivative to consider the frequency-, temperature-, and strain-level- sensitivities of VE materials, $a_v^{(n)}$, $b_v^{(n)}$ and $G^{(n)}$ are determined based on the corresponding shift factors $\lambda_0^{(n)}$, $\lambda_1^{(n)}$ and $\lambda_2^{(n)}$, i.e.,

$$a_v^{(n)} = a_{ref} (\lambda_0^{(n)})^\alpha, \quad b_v^{(n)} = b_{ref} (\lambda_0^{(n)})^\alpha \lambda_1^{(n)}$$

$$\text{and } G^{(n)} = G \lambda_2^{(n)}, \quad (3a - c)$$

$$\lambda_0^{(n)} = \exp \left[-p_1 \left(\bar{\theta}_v^{(n)} - \theta_{ref} \right) / \left(p_2 + \bar{\theta}_v^{(n)} - \theta_{ref} \right) \right]$$

$$\text{and } \bar{\theta}_v^{(n)} = \frac{1}{2d_v} \left(\theta_{j_a}^{(n)} d_v + \theta_{j_b}^{(n)} d_v \right), \quad (4a, b)$$

$$\lambda_1^{(n)} = 1 + C_1 (\gamma_{max}^{(n)} - 1) \geq 1$$

$$\text{and } \lambda_2^{(n)} = 1 + C_2 (\gamma_{max}^{(n)} - 1) \geq 1, \quad (5a, b)$$

where $C_1 = 0.124$ and $C_2 = -0.182$ are coefficients obtained

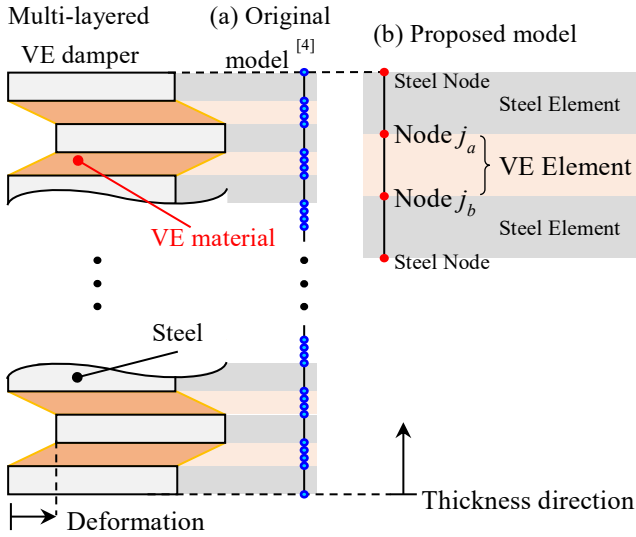


Figure 4. The original [4] and the proposed simplified modeling approaches for multi-layered VE dampers.

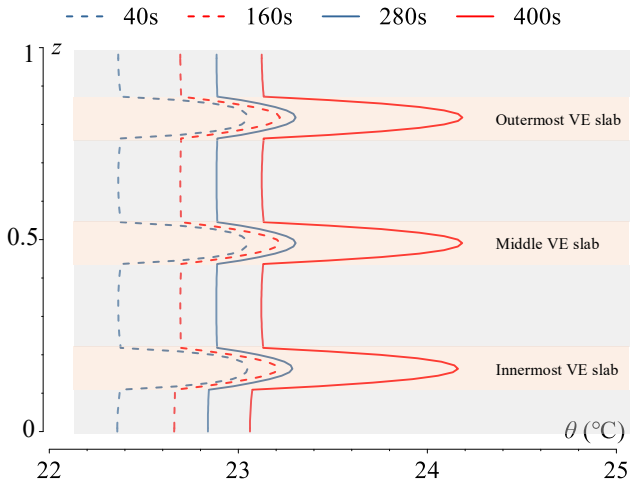


Figure 5. Temperature distributions within multi-layered VE dampers (Along-wind direction loading).

from several tests [8], $\gamma_{max}^{(n)}$ = history peak value among the strain levels $\gamma_d^{(n)}$ ($= u_d^{(n)} / d_v$) for time step from 1 to n using $u_d^{(n)}$ = damper deformation and d_v = VE material thickness.

In the next Dynamic analysis [3], by considering Eq. 3 and the known uniform shear strain $\gamma_d^{(n)}$, the unknown shear stress $\tau_v^{(n)}$ in Eq. 2 can be solved as

$$\tau_v^{(n)} = \frac{G^{(n)} \gamma_d^{(n)} [(\Delta t)^\alpha + b_v^{(n)} w^{(0)}]}{[(\Delta t)^\alpha + a_v^{(n)} w^{(0)}]} + \frac{G^{(n)} b_v^{(n)} \sum_{i=1}^N w^{(i)} \gamma_d^{(i)} \gamma_d^{(n-i)}}{[(\Delta t)^\alpha + a_v^{(n)} w^{(0)}]} - \frac{a_v^{(n)} \sum_{i=1}^N w^{(i)} \tau_v^{(i)}}{[(\Delta t)^\alpha + a_v^{(n)} w^{(0)}]}. \quad (6)$$

From the above calculations of stress-strain relationship, the global damper reaction force $F_d^{(n)}$ is estimated by multiplying the total shear area A_s and shear stress, i.e.,

$$F_d^{(n)} = A_s \tau_v^{(n)}. \quad (7)$$

Meanwhile, using the calculated $\tau_v^{(n)}$ and $\gamma_d^{(n)}$, the dissipated energy density can be calculated as

$$\Delta W_d^{(n)} = (\tau_v^{(n)} + \tau_v^{(n-1)}) (\gamma_d^{(n)} - \gamma_d^{(n-1)}) / 2. \quad (8)$$

Next, the nodal temperature-rise $\Delta \hat{\theta}_j^{(n)}$ due to $\Delta W_d^{(n)}$ at the end of time step n is calculated in the VE slab as:

$$\Delta \hat{\theta}_j^{(n)} = (\Delta W_d^{(n)} / s\rho) / 2, \quad \text{for } j=j_a \text{ and } j_b, \quad (9)$$

where $s\rho$ = the product of the VE element specific heat capacity and density.

The nodal temperature $\theta_j^{(n+1)}$ for next time step $n+1$ is set by combing the nodal temperature-rise $\Delta \hat{\theta}_j^{(n)}$ and the nodal temperature $\hat{\theta}_j^{(n)}$ obtained from the 1D heat transfer analysis [1], i.e.,

$$\theta_j^{(n+1)} = \begin{cases} \hat{\theta}_j^{(n)} + \Delta \hat{\theta}_j^{(n)}, & \text{for VE nodes } (j=j_a \text{ and } j_b) \\ \hat{\theta}_j^{(n)}, & \text{for steel nodes} \end{cases}. \quad (10)$$

The above procedure is repeated for subsequent time steps.

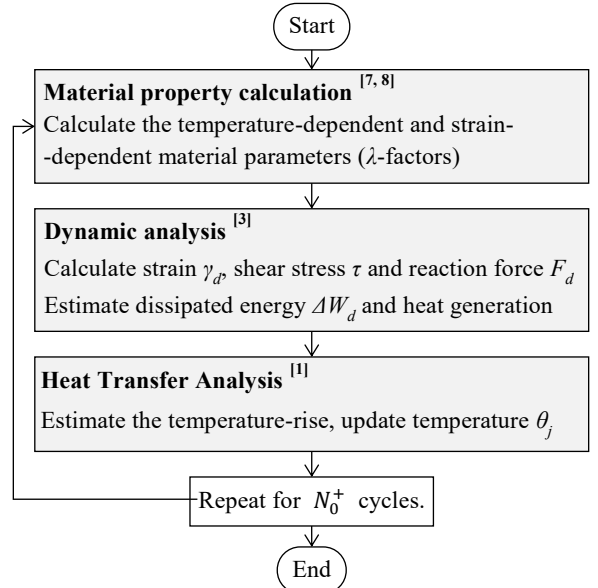


Figure 6. Flowchart of the 1D time-history analysis.

4. VERIFICATION OF SIMPLIFIED MODELING APPROACH

Using the proposed model, the 1D time-history analysis was carried out to simulate the VE damper behavior under the test loading condition [5]. The accuracy is verified through comparison to both test and original model results. Since loading duration (400 s) is short and the full-scale VE damper has large capacity, the heat dispersed from the VE damper to air was ignored in the heat transfer analysis [1].

Fig. 7 shows the temperature time-histories and $F_d - u_d$ hysteresis curves from proposed model, test and original model in along- and across-wind directions. The temperature results from proposed model are the weighted average values (Eq. 4b), fitting well with the average values from eight thermocouples (test results) and 3×12 VE nodes (original model results), respectively. The hysteresis curves from proposed model also have good agreement with test results, indicating good accuracy of the proposed model in predicting the behavior of the multi-layered VE damper.

To verify the effectiveness of the proposed model, this chapter compared its calculation time with the original model in Table 1. In along-wind direction, the dynamic analysis time decreased from 139.64 to 60.26 s (proposed/original ratio = 0.43), while the heat transfer analysis showed a more significant improvement, from 17.18 to 0.68 s (ratio = 0.04). Overall, the total time was reduced to 0.39 of the original time.

Similar improvements were observed in the across-wind direction, confirming the computational efficiency of the proposed model.

5. CONCLUSIONS

This study proposes a simplified modeling approach for multi-layered VE dampers that significantly improves computational effectiveness while maintaining accuracy. The proposed model accurately reproduces test results for temperature response under wind-induced random loading. Furthermore, it provides comparable accuracy to detailed original model [4] while reducing computational time by approximately 60%. This reduction in computation time is particularly significant in dynamic and heat transfer analysis.

References

- [1] Kasai K, Sato D, Huang YH. Analytical methods for viscoelastic damper considering heat generation, conduction and transfer under long-duration cyclic load. *J Struct Constr Eng* 2006; 599:61–9 (In Japanese).
- [2] Osabel DM, Sato D, Kasai K. Evaluation Method for Viscoelastic Damper subjected to Long-Duration Wind Loading by Equivalent Sinusoidal Waves, National Symposium on Wind Engineering Proceedings, 2020, Volume 26, Vol.26 (2020), Pages 102-107.
- [3] Kasai K, Osabel DM, Sato D. Dynamic response characterization and simplified analysis methods for viscoelastic dampers considering heat transfer. *Earthquake Engng Struct Dyn*. 2023; 52: 27–50.
- [4] Sato D, Liang Q and Osabel DM. Three-Dimensional Finite Element Analysis and Simplified One-Dimensional Analysis Methods for Full-Scale Viscoelastic Damper Considering Strain Sensitivity. *Earthquake Engng Struct Dyn*. 2024; 0098-8847.
- [5] Sato D, Kasai K, Sugiyama N, Matsuda K. Simplified Performance Evaluation Tests of Full-scale Viscoelastic Damper under Wind-induced Response, Summaries to Technical Papers of Annual Meeting 2015, Japan Association for Wind Engineering, Pages 189-190 (In Japanese)
- [6] Architectural Institute of Japan. Recommendations for Loads on Buildings, Maruzen, 2004. 9. (In Japanese).
- [7] Kasai K, Teramoto M, Okuma K, Tokoro K. Constitutive rule for viscoelastic materials considering temperature and frequency sensitivity (Part 1: Linear model with temperature and frequency sensitiveness). *J Struct Constr Eng, AIJ*. 2001; 543:77-86 (In Japanese).
- [8] Kasai K, Teramoto M, Okuma K, Tokoro K. Constitutive rule for viscoelastic materials considering temperature and frequency sensitivity (Part 2: Nonlinear model based on temperature-rise, strain and strain-rate). *J. Struct. Constr. Eng., AIJ*. 2002; 561:55-63 (In Japanese).

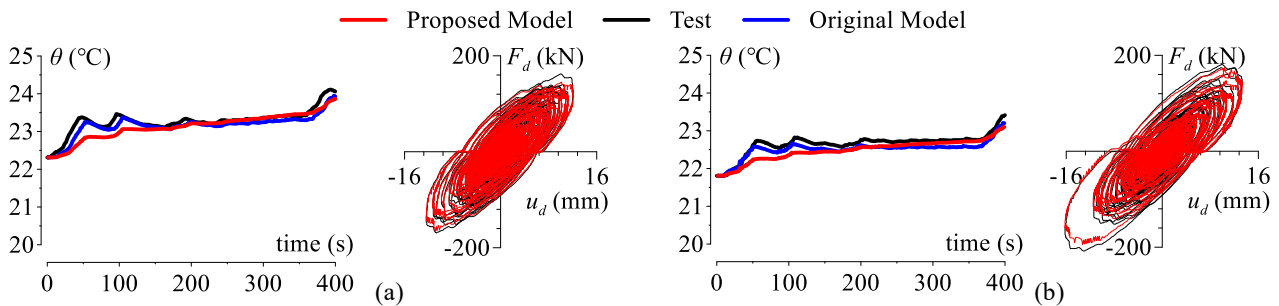


Figure 7. Temperature time-history results and $F_d - u_d$ hysteresis curve under (a) along-wind direction and (b) across-wind direction from proposed model, test and original model.

Table 1. Calculation time using proposed model and original model in along- and across-wind directions

Wind direction	Along-wind			Across-wind		
	Proposed	Original	Proposed/Original	Proposed	Original	Proposed/Original
Material property calculation	0.55	2.03	0.27	0.59	1.80	0.33
Dynamic analysis	60.26	139.64	0.43	59.41	130.28	0.46
Heat transfer analysis	0.68	17.18	0.04	0.65	16.23	0.04
Total time	63.77	163.15	0.39	62.98	150.17	0.42

*1 東京科学大学 大学院生

*2 東京科学大学 准教授・博士 (工学)

*3 チョンナム大学 韓国 博士研究員

* Graduate Student, Institute of Science Tokyo *¹

* Associate Professor, IIR, Institute of Science Tokyo, Dr. Eng.*²

* Postdoctoral Researcher, Chonnam National University, South Korea, Ph.D.*³